Turkish Journal of Electrical Engineering & Computer Sciences

http://journals.tubitak.gov.tr/elektrik/

Research Article

Turk J Elec Eng & Comp Sci
(2018) 26: 11 – 22

doi:10.3906/elk-1705-16

Automatic detection of the respiratory cycle from recorded, single-channel sounds from lungs

Selim ARAS*, **Mehmet ÖZTÜRK**, **Ali GANGAL**
Department of Electrical and Electronics Engineering, Faculty of Engineering, Karadeniz Technical University, Trabzon, Turkey

Received: 02.05.2017 • **Accepted/Published Online:** 14.11.2017 • **Final Version:** 26.01.2018

Abstract: Listening to the sounds made by the lungs is a long-standing method that is still used to diagnose lung diseases. Many studies have been conducted on the automatic recognition of recorded sounds from the lungs. However, in these studies, respiratory cycles, i.e. inhalations followed by exhalations, were either monitored manually or by using multichannel signals of the sounds made by the lungs. In order to recognize sounds made by the lungs automatically, one must first use these sounds to determine the respiratory cycles. Our previous study was the first study presented in the literature in which the boundaries of respiratory cycles were determined based on single-channel sounds from the lungs. However, this method was not successful when ambient noise occurred and interfered with the sounds from the lungs. In the present study, a new method has been developed in which important changes were made to reduce or negate the effects of ambient noises. Our proposed new method includes a processing method that we developed to obtain respiratory cycles as smooth, repetitive patterns. Then the dynamic time-warping algorithm was used to determine the boundaries of the respiratory cycles, based on the similarity of the patterns. This new method was used to detect the seven sounds that are commonly made by the lung. As a result, the limits of the respiratory cycles were obtained with a mean absolute error of 56.51 ms. In addition, the method we developed has the potential to determine the boundaries of the patterns in signals that contain repetitive data, such as the sounds made by the lungs in this study.

Key words: Respiratory cycle, sounds of lungs, electronic auscultation, repetitive pattern, dynamic time warping

1. Introduction

Auscultation is the process of using a stethoscope to listen to the sounds that emanate from within the human body, including sounds from the heart, lungs, and gastrointestinal tract. Since Laënnec invented the stethoscope in 1816, this instrument has undergone very little change. The modern stethoscope was modernized by David Litmann in 1960 [1]. Today, sounds from the lungs can be recorded with electronic stethoscopes and transferred to a computer for detailed analysis. The professional that interprets sounds from the lungs during auscultation must have good hearing and expertise in using the process. Current electronic stethoscopes can detect low-frequency sounds that are difficult for the human ear to detect. Many studies have been conducted on the automatic detection of sounds from the lungs; however, the results of these studies cannot be compared due to several limitations, including lack of a common data set, presence of sounds other than sounds from the lungs, and use of different standards for acquiring and analyzing the sounds [2,3].

Sounds from the lungs naturally have complex structures, because the passage of gases through the respiratory system causes the walls of the airways to vibrate [4]. Thus, the variety of sounds emanating from

*Correspondence: saras@ktu.edu.tr

the lungs and the boundary points of respiratory cycles cannot be detected adequately with the methods of conventional zero-crossing and energy-thresholding that are used to detect voice zones [2]. Researchers have tried to detect the boundary points of respiratory cycles by using different types of signals such as sounds from the trachea [5], sounds of flowing air [6], placing a microphone on the side of the nose to detect sounds [7], obtaining a photoplethysmogram [8], and obtaining a signal from a piezoresistive belt sensor [9]. In these studies, different data were considered to improve the detection of the boundary points of respiratory cycles or breathing frequencies. Additionally, several studies have defined the boundary points of respiratory cycles based on different signals that were recorded simultaneously for different sounds from the lungs. Various sound signals have been used in studies with healthy individuals, which were recorded at the same time as sounds from the lungs. These nonlung sound signals included signals from the trachea [10], signals from a microphone placed on the side of the nose [11], and signals due to chest movements recorded with a smartphone camera [12]. For people with sleep apnea, sound signals from the lungs and the trachea have been recorded simultaneously [13], and airflow signals were obtained from a group of healthy people, a group with abnormal breathing [14], and a group with asthma [15]. These studies had to acquire multichannel data to detect respiratory cycles using the sounds from the lungs. Since acquiring multichannel data requires both time and effort, it is a bit more complex than auscultation, which is a relatively simple process. Therefore, it is necessary to focus on single-channel sounds from the lungs that can be used by physicians to detect respiratory cycles.

Few studies have used single-channel sounds from the lungs. Mondal et al. [4] detected the boundary points of respiratory cycles using single-channel sounds from the lungs obtained from a group of people, some of whom could breathe normally and some of whom had chronic obstructive pulmonary disease. The researchers attempted to obtain a complete respiratory cycle based on the sound data from multiple breaths by using an algorithm that was based on the Hilbert transform. Le Cam et al. [16] proposed a statistical method to perceive the respiratory phase from the sounds made by the lungs of healthy people, but they failed to provide information about the method they used to record the sounds. To the best of our knowledge, our previous work [2] was the first to determine the limits of respiratory cycles from single-channel recorded sounds from the lungs. However, the success of the method was diminished by the extraneous peaks caused by the noise. In this study, significant changes are made to the previous method in order to automatically detect the boundaries of the breath cycle from the sounds made by the lungs in the presence of noise. In addition, the entire process that is used in our new method is presented in detail. The first part of the process, i.e. the preprocessing method, described in Section 2.2, is developed to obtain respiratory patterns as repetitive patterns and is applied to the sounds from the lungs. The second part of the process, described in Section 2.3, was developed to identify the boundaries of the patterns that represent the respiratory cycles and compare the similarities of these patterns in the dynamic time warping (DTW) algorithm. Unlike our previous method, the Hamming window function is used in the preprocessing step, instead of the triangle window function, to obtain more accurate boundaries of the respiratory cycles. In addition, in our new method, the amplitudes of the sounds are normalized in each pattern selected for comparison using the DTW algorithm. Thus, the results of the comparisons of similar patterns were affected less by differences in the amplitudes. Another important difference is that, in our previous method, we compared the points in the N_s number of points selected in the DTW algorithm instead of comparing the minimum and maximum points of the pattern selected from the preprocessed signal. Thus, it was ensured that the peaks caused by noise had less effect on the success of the method. The performance of our new method is evaluated with many common sounds, including the wheezing sound, healthy breathing sounds, fine crackle sounds, and coarse crackle sounds, as well as rhonchi, pleural friction rub, and bronchial breathing sounds. Additionally, the performance is analyzed with additive white Gaussian noise (AWGN) to the fine crackle sound from the lungs, because fine crackle sound is more prone to deterioration with noise. The results of the method are compared with the boundaries of patterns that have been determined manually by physicians.

2. Materials and methods

For the implementation of the method, the original signal and an exact copy of the original signal are needed. Therefore, a copy of the original signal was used to determine the boundaries of the respiratory cycles in the sounds from the lungs. The aim here was to ensure that the methods that result in data losses when applied to the original signal can be applied successfully to a copy of the signal. The boundaries of the respiratory cycles determined in the copy of the signal were the same as the boundaries of the respiratory cycles in the original signal. With the proposed method, respiratory cycles can be determined automatically from single-channel sounds from the lungs. Thus, real-time applications can be realized. In our proposed method, the preprocessing method described in Section 2.2 was developed to obtain respiratory cycles as smooth, recurring patterns. Since each repetitive pattern represents a respiratory cycle, the boundaries between these patterns are concurrently the boundaries of the respiratory cycle. A new algorithm was developed using the similarity of the patterns and the DTW algorithm to determine the boundary points of the repetitive patterns, and this algorithm is presented in Section 2.3.

2.1. Sounds from the lungs and data collection

The American Thoracic Society has classified commonly heard sounds from lungs as healthy sounds, fine crackles, coarse crackles, wheezing, and rhonchus [1]. In our study, we recorded seven different sounds, i.e. the five sounds mentioned above, bronchial breathing sound, and pleural friction rub. The study was conducted with the approval of the Research Ethics Committee, Karadeniz Technical University. We used a single-channel electronic stethoscope (Thinklabs ds32a+) that had a digital sound recorder connected to its analogue output. Recordings were made in accordance with the auscultation procedure in a hospital environment with ambient noise. Each record contains a minimum of three respiratory cycles. All the recordings were obtained from patients at the Department of Chest Diseases, Karadeniz Technical University. The sounds were recorded by two specialists and were labeled with the decision they agreed on. Recordings were taken from three different individuals for each sound type. That is, lung sound recordings were taken from 21 different individuals in total for each sound type.

2.2. Preprocessing

In order to obtain the spectrogram in the preprocessing, we first applied Fourier transform to the signal. Let $x[n]$ be a discrete signal of length N and $w[n]$ a windowing function (Hamming window here) of the same length. Then, the N-point, windowed, discrete Fourier transform of $x[n]$ is

$$X[n,k] = \sum_{m=-\infty}^{\infty} x[m]\, w[n-m]\, e^{-\frac{j2\pi km}{N}}, \tag{1}$$

where j is the square root of –1, $n = 0, \ldots, N \, and \, k = 0, \ldots, N-1$.

$$w[n] = \begin{cases} 0.54 - 0.46\cos\left(\frac{2\pi n}{N_w}\right), & 0 \le n \le N_w - 1 \\ 0, & N_w - 1 < n < 0 \end{cases} \tag{2}$$

The Hamming window, $w[n]$ (given in Eq. (2)), is assumed to be nonzero only in an interval with length N_w, and is referred to as the analysis window. Consider sliding the $w[n]$ along with L samples, rather than one sample at a time, and a matrix will be obtained that is called the spectrogram of $x[n]$. After calculating the spectrogram, the next step is the calculation of the mean energy (Eq. 3) over the $X[n,k]$ between f_L (80 Hz) and f_H (1000 Hz).

$$p[n] = \frac{1}{f_H - f_L} \sum_{i=f_{LH}}^{f} |X[n,i]|^2 \tag{3}$$

For example, in the p[n] signal in Figure 1, there is a noise effect between the two respiratory cycles (outlined with a yellow frame). In order to prevent this type of disruption and have a smoother energy distribution graph, the band-passed mean energy, $p[n]$, is smoothed with the smoothing function presented in [17]:

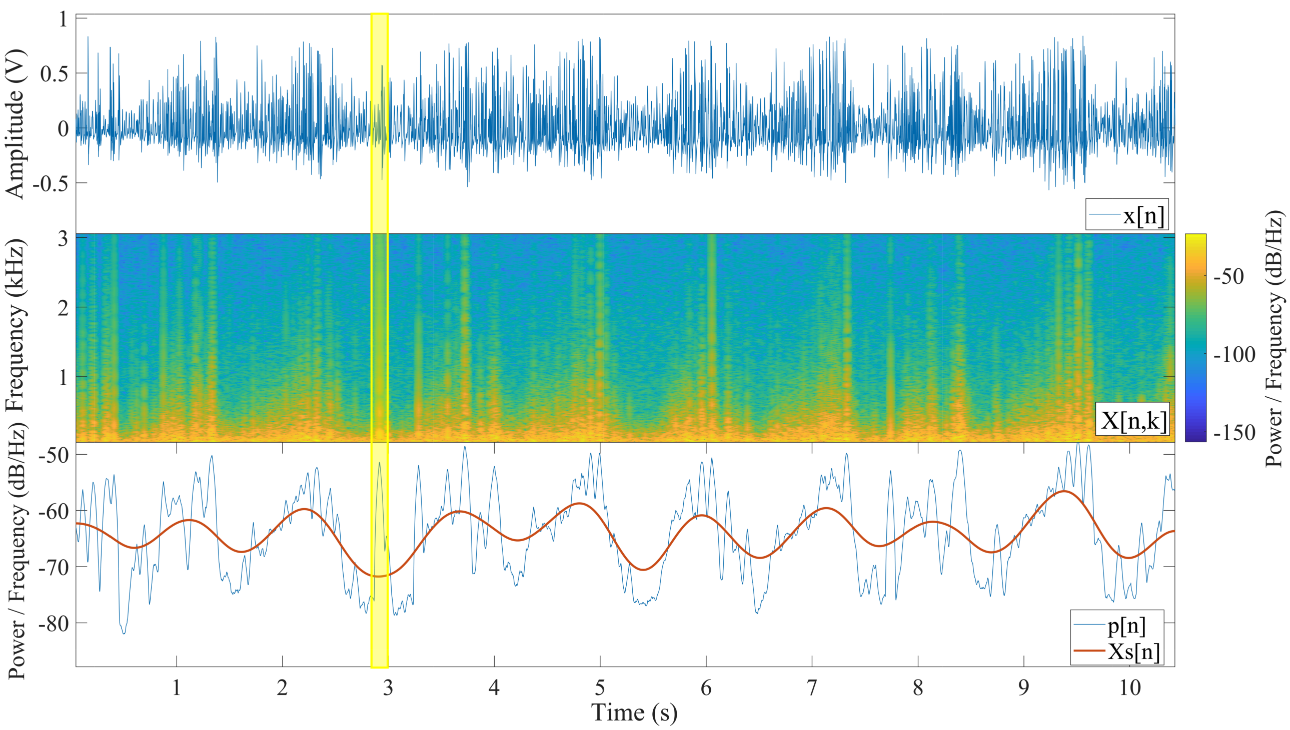

Figure 1. From top to bottom: waveform, spectrogram, and bandpass filtered mean energy with smoothed version of a pleural friction rub sound.

$$X_s[n] = smooth(p[n]) \tag{4}$$

The smoothed energy signal contains local minimum points that may be represented as the boundary points of respiratory cycles. Local minimum points are calculated from the roots of the first derivative of $X_s[n]$, where the second derivative is positive:

$$\min Ind[j] = \frac{dX_s[n]}{dn} = 0, \quad \text{where } \frac{d^2X_s[n]}{dn^2} > 0 \tag{5}$$

2.3. Identification of boundary points from repetitive patterns

Figure 1 shows the preprocessing using a pleural friction rub sound. When the $X_s[n]$ signal, obtained after the preprocessing, is examined, the respiratory cycles appear as repetitive, smooth patterns with two peaks. The boundary points of the respiratory cycles correspond to the minimum points of these patterns. Our proposed method takes advantage of the minimum points of the $X_s[n]$ signal and the similarity of the respiratory cycles to determine the boundary points.

The first step is the determination of model $(M_i[n])$ and test patterns $(T_{i,p}[n])$, which separately represent the respiratory cycles. As an example of the process of obtaining the boundaries of the respiratory cycle, Figure 2 shows the determination phase of the model, the test patterns, and the corresponding indices.

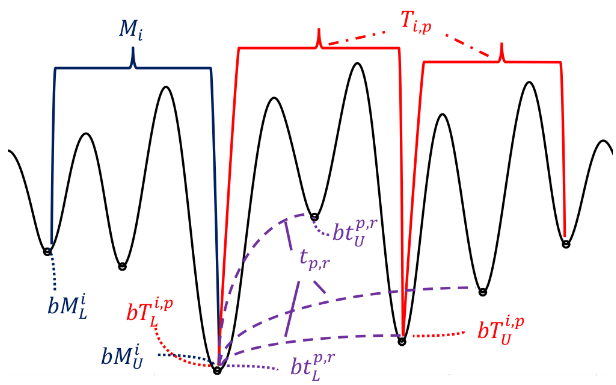

Figure 2. Process of determining a model pattern and test patterns.

The boundaries of all possible model and test patterns are selected from the $\min Ind$ obtained in Eq. (5). If the lower and upper bounds of the ith model are expressed as bM_L^i and bM_U^i, respectively, the upper and lower bounds of the model can be selected in the range $1 \leq bM_L^i \leq bM_U^i \leq 2L_{\max}$. A pattern that represents a respiratory cycle and can be selected as a model must be in this range. A value of $L_{\max}$ should be selected that is larger than the longest possible respiratory cycle, i.e. $L_{\max} = 5.5$ s in this study. The length of the selected model pattern should be in the range of $L_{\min} \leq bM_U^i - bM_L^i \leq L_{\max}$. This limitation is necessary to reduce the complexity of the process by controlling the possible lengths of the model pattern. The selected value of $L_{\min}$ should be shorter than the shortest possible respiratory cycle, i.e. $L_{\min} = 1.25$ s in this study. Taking all these conditions into consideration, for the ith model the lower boundary index, bM_L^i, is calculated from the following function:

$$f\left(bM_L^i\right) = \begin{cases} \min Ind[1], & i = 1 \\ bM_U^{i-1}, & i > 1 \end{cases} \tag{6}$$

The ith model's upper limit, bM_U^i, is determined within the above limits, depending on the value of bM_L^i. Thus, samples of the signal $X_s[n]$ in the range $bM_L^i \leq n \leq bM_U^i$ are determined as model patterns. However, since there will be a large number of samples in the selected range, the process of comparing similarities in the DTW algorithm is complex. In order to reduce the complexity of the process, N_s numbers of evenly distributed samples are taken from the model in a process known as decimation. Here number N_s was chosen to be at least twice the maximum frequency of the $X_s[n]$ signal, in accordance with the sampling theory. Then the amplitudes of these samples were normalized to prevent the DTW algorithm from producing incorrect results because of the differences in the amplitudes between the patterns. Once the lower bound, bM_L^i, and upper bound, bM_U^i, of the model have been determined, the coefficients that represent the ith model are calculated from the following equation with $n = 1, \ldots, N_s$;

$$M_i[n] = \frac{X_s\left(round\left(bM_L^i + n\left(\frac{bM_U^i - bM_L^i}{N_s - 1}\right)\right)\right)}{X_{sm}^i}, \tag{7}$$

where X_{sm}^i is the maximum of the amplitude values between the bM_U^i and bM_L^i indices of the X_s. The next step is to specify test pattern samples to be compared with $M_i[n]$. Each test pattern $(T_{i,p}[n])$ is selected from subtest patterns $(t_{p,r}[n])$ that have the same lower bound. The lower bound of the first test pattern, $(bt_L^{p,r})$, to be determined after the model pattern, will be equal to the upper bound of that model (bM_U^i). By keeping $bt_L^{p,r}$ constant, r numbers of subtest patterns that match the $L_{\min} \le bt_U^{p,r} - bt_L^{p,r} \le L_{\max}$ condition are determined. Additionally, amplitude normalization is performed for each subtest pattern in the same manner as the model pattern, and N_s samples are selected from each pattern. Then these samples are compared with $M_i[n]$ in the DTW algorithm. The subtest pattern with the smallest value obtained from DTW is determined as the first test pattern $T_{i,p}[n]$ after the model. The next step is to identify a new test pattern that is similar to the model pattern selected previously. To do so, the index of the upper bound of the last test pattern determined is considered to be the index of the lower bound of the new test pattern, and the same operation continues until the end of the $X_s[n]$ signal, as long as the conditions stated before are satisfied. The indices of the lower limit of the subtest patterns $(t_{p,r}[n])$, which are selected to determine the pth test pattern of the ith model $(T_{i,p}[n])$, are calculated as follows:

$$f\left(bt_L^{p,r}\right) = \begin{cases} bM_U^i, & p = 1 \\ bt_L^{i,p-1}, & p > 1 \end{cases}, \tag{8}$$

where r is the number of subtest patterns. After the upper bound index of the rth test pattern is determined according to the $L_{\min} \le bt_U^{p,r} - bt_L^{p,r} \le L_{\max}$ condition, the rth test pattern to be formed to determine the pth test pattern candidate is calculated with the following equation:

$$t_{p,r}[n] = \frac{X_s\left(round\left(bt_L^i + n\left(\frac{bt_U^i - bt_L^i}{N_s - 1}\right)\right)\right)}{X_{st}^i}, \tag{9}$$

where X_{st}^i is the maximum amplitude value between the bt_U^i and bt_L^i indices of X_s. The determined r number of the subtest patterns is compared with $M_i[n]$ using the DTW algorithm. Then the boundaries of the subtest pattern with the minimum comparison results are determined as the upper and lower bounds $(bT_L^{i,p}, bT_U^{i,p})$ of the first test pattern, $T_{i,p}[n]$.

The next step is to determine a new test pattern that is similar to the model we selected. The upper boundary index of the last test pattern is considered as the lower boundary index of the new test pattern to be determined, and the same operations continue until the end of the $X_s[n]$ signal, as long as the conditions are satisfied. The same process is repeated for the next model to be identified. After the indices of all possible models and test patterns have been determined, the mean DTW comparison results of all the test patterns, determined to resemble the model pattern, are calculated. Among all the models, the limits of the model with the lowest mean DTW and its test patterns are considered to be the limits of the lungs' respiratory cycles.

2.4. Dynamic time warping

With the DTW method, the closest elements of the vectors are matched to each other, ensuring that the sum of the distances can be kept at the smallest possible value. Taking an equal number of samples with equal intervals from the patterns defined as a model provides the data that were compared in the DTW algorithm. If we define the data obtained from the model and the test patterns as $(m_1, \ldots, m_M)$ and $(t_1, \ldots, t_N)$ vectors, respectively, the distance between these two vectors $D(MN)$ with the DTW algorithm is calculated as follows [18]:

$$D(i,j) = \min \left\{ \begin{array}{l} D(i, j-1) \\ D(i-1, j) \\ D(i-1, j-1) \end{array} \right\} + d(m_i + t_j), \tag{10}$$

where $M = N = N_s$ is the number of samples taken from the model and the test pattern with equal intervals, $i = 1, \ldots, M$, and $j = 1, \ldots, N$. In the equation above, $d(mt)$ is the local distance function and is calculated with Eq. (11):

$$d(m,t) = \sqrt{\sum\nolimits_i (m_i + t_i)^2} \tag{11}$$

A flow chart that summarizes our proposed method is presented in Figure 3.

3. Results and discussion

The method we developed to determine the boundaries of the respiratory cycles of single-channel sounds from lungs was applied to the entire data set. The results obtained for seven different sounds from lungs are presented in Figure 4.

In Figure 4, the red dots represent the lower and upper boundary points of the respiratory cycles that were obtained with the proposed method. The magenta vertical lines represent the boundaries of the respiratory cycles determined by physicians. The results in Figure 3 indicate that the bounds determined with our proposed method are very close to the boundaries set by the physicians. In addition, the physicians listened to the respiratory cycles between the boundary points determined by our method and concluded that they were appropriate. For another perspective, the proposed method and the results of the bounds determined by the physicians are compared statistically in the Table.

Furthermore, Figure 4 shows the effect of the amplitude normalization applied to each pattern to minimize the effect of the amplitude differences of the patterns. In our previous method, the minimum and maximum peaks were used to compare the similarities of the models. In the proposed method, equal numbers of samples from normalized patterns were compared and the success rate was increased. A suitable example of this is shown in the sixth respiration pattern of rhonchi in Figure 4. Although these patterns have different numbers of peaks, our proposed method determined the boundary points successfully. In addition, the fact that the respiratory cycles determined by our method were accepted by the physicians is a factor that supports the success of the proposed method.

The statistical results of the proposed method are presented in the Table, and can be used to evaluate the success of the proposed method from another perspective.

The duration of a respiratory cycle depends on the type of disease the patient has, and this is reflected in the average duration of the respiratory cycles. Wheezing is a sound that occurs in the lungs as a result of the restricted movement of air caused by the constriction of the small airways in the lungs. Therefore, wheezing has

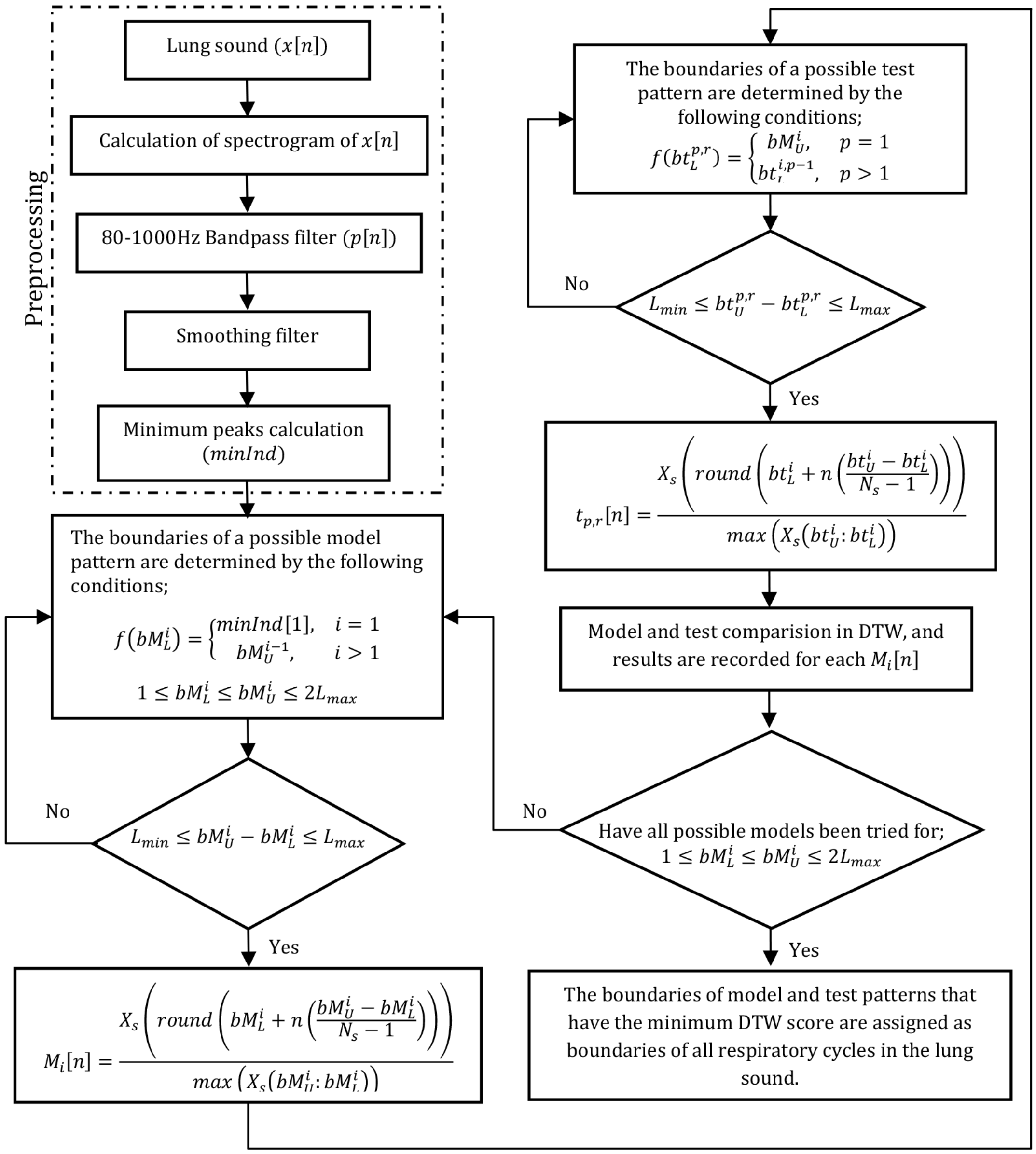

Figure 3. Flow chart of the proposed method.

the highest mean duration in the respiratory cycle (3510.82 ms). Obtaining low duration values of the mean absolute error shows the success of our proposed method. The bronchial breathing sound is the sound heard due to the accumulation of fluid in the lungs. As the respiratory quality decreases due to the accumulated fluid, the patient must breathe more frequently. Therefore, bronchial breathing sound has the shortest duration of the mean respiratory cycle (2033.97 ms).

When we examined the means of all our results, the mean duration of all respiratory cycles was 2677.43 ms, and the mean absolute error of the durations was approximately 120 ms. When these two values were compared, the mean absolute error of the durations was approximately 4.4% of the mean duration of the respiratory cycles. This value is a very important factor in measuring the success of our proposed method, because the loss of data was quite low compared to the entire breathing cycle. In addition, the mean absolute

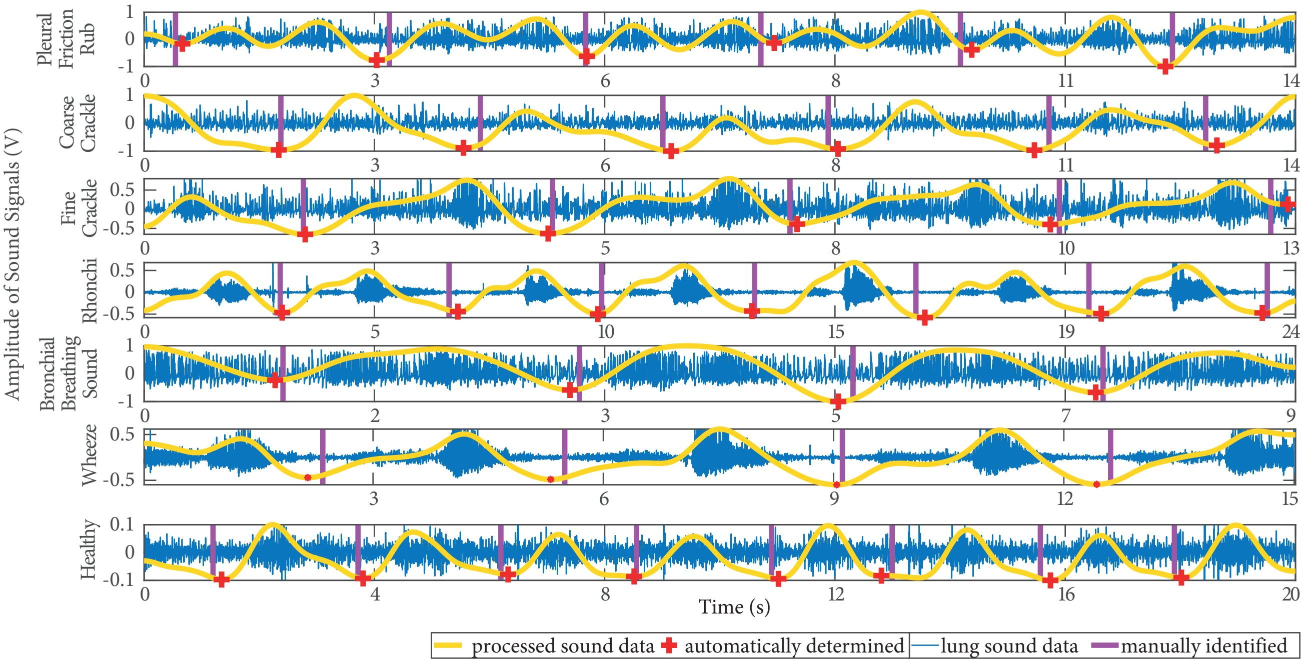

Figure 4. Results of the proposed method on seven different lung sounds.

Table. Statistical comparisons of respiratory boundary points defined manually and automatically.

Lung sound type	Mean respiratory cycles (ms)	Standard deviation of respiratory cycles (ms)	Mean absolute errors (ms)	Standard deviation of absolute error (ms)
Pleural friction rub	2355.79	100.14	105.06	55.43
Fine crackle	2738.73	75.85	88.32	65.70
Coarse crackle	2245.58	184.39	125.43	62.06
Rhonchi	3437.23	304.32	130.86	81.20
Bronchial breathing	2033.97	143.11	72.43	25.22
Wheeze	3510.82	289.96	180.60	58.39
Healthy	2419.90	358.76	128.29	47.54
Mean of results	2677.43	208.08	118.71	56.51

error rates vary between 3.2% and 5.6%. It is possible to say that these error rates are within acceptable limits for the automatic respiratory cycle detection applications, when the measuring errors, which may occur at manual respiratory cycle boundary determination by physicians, are taken into consideration.

The standard deviation of the absolute error rates may appear higher than expected for the mean values. However, it is reasonable that the standard deviations would be higher than expected, because the results of our method were evaluated according to the boundaries set by the physicians. Their boundaries took into account that the duration between breathing cycles is short for some types of sounds from the lungs and long for other types of sounds. Thus, the small shifts at the boundary points determined by the physicians resulted in an increase in the standard deviation.

Figure 5 compares the results of our previous work with the results of the proposed method, based on an example of a fine crackle sound from the lungs.

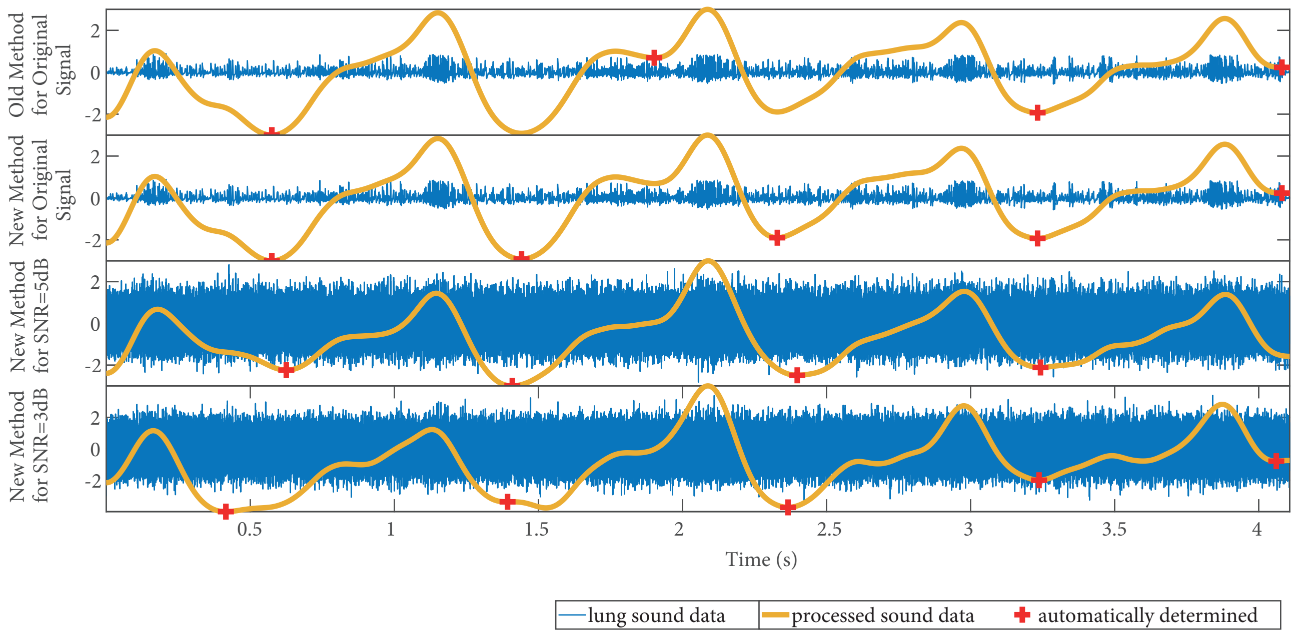

Figure 5. Comparison of our earlier method and the proposed method.

The red dots show the boundaries set by the methods. Due to the extra peaks, shifts occurred at the boundary points that had been determined with our previous method. Our proposed method determined the boundary points appropriately, even though there were different amplitudes and extra peaks. The performance of the method in the presence of noise was tested with AWGN noise added to the signal (signal-to-noise ratios of 3 and 5 dB). These results are shown at the bottom of Figure 5. Even though it was very difficult to hear the sounds of respiration due to the added noise, and despite the distortions in the patterns, the results showed that the proposed method had a high ability to determine the boundaries.

Many previous studies for determining the breathing cycles were performed in multichannel mode. Since our proposed study was developed for single-channel sounds from the lungs, it would be more appropriate to compare the results with the results of studies using a single-channel acoustic signal. In an outstanding work in this area, Jin et al. [19] recorded tracheal breath sounds from 7 healthy individuals and 14 airway obstruction individuals (unspecified voice types). Using the phase shift difference information method, 98.07% accuracy was obtained. Yadollahi et al. [20] used a linear model based on the entropy of the tracheal voice for the data they received from 10 healthy individuals. They reported that this entropy-based model followed the tracheal voice change with a 9% error. In our proposed study, it was not necessary to record sounds from the lungs in a specific area, such as the trachea, which means that it is not important what kind of sounds from the lungs are recorded or where. This is another positive contribution of our method, namely that sounds from the lungs only need to be recorded from appropriate regions according to the auscultation procedure. Our method has yielded quite successful results on seven commonly encountered sounds from the lungs. This shows the potential of this method to be successful in all types of sounds from the lungs.

4. Conclusion

In this study, we proposed a method that automatically determines the limits of respiratory cycles for all types of sounds from the lungs without requiring manual user interaction. The most important feature of this method is being fully automatic. Another important feature, which distinguishes this method from other studies, is that it was applied successfully to single-channel sounds from lungs. This was possible because auscultation is essentially a one-channel process. Since the proposed method can determine respiratory cycles successfully, each of the automatically determined respiratory cycles can be used for training or as test data in classification studies. This gives us the opportunity to work with fully automated recognition of single-channel sounds from the lungs, which is a significant benefit provided by our proposed method. Moreover, the method has the potential to be applied successfully to each type of signal in which repetitive patterns occur. However, for real-time applications, studies should be conducted to determine the $L_{\min}$ and $L_{\max}$ parameters dynamically.

Our future studies will include offline classification studies for the automatic detection of sounds from lungs. Studies will be conducted to develop algorithms that can extract and classify features, thereby achieving the automatic determination of the training and test clusters. The successful results obtained from these studies will be followed by studies designed to provide real-time recognition of sounds from the lungs.

Acknowledgments

The authors thank the physicians responsible for the recordings and the patients who participated in this study. This work was supported by the Scientific and Technological Research Council of Turkey (TÜBİTAK) (Project No. EEEAG- 116E003).

References

[1] Lakhe A, Sodhi I, Warrier J, Sinha V. Development of digital stethoscope for telemedicine. J Med Eng Technol 2016; 40: 20-24.

[2] Aras S, Özturk M, Gangal A. Endpoint detection of lung sounds for electronic auscultation. In: IEEE 2016 International Conference on Telecommunications and Signal Processing; 27–29 June 2016; Vienna, Austria. New York, NY, USA: IEEE. pp. 405-408.

[3] Gurung A, Scrafford CG, Tielsch JM, Levine OS, Checkley W. Computerized lung sound analysis as diagnostic aid for the detection of abnormal lung sounds: a systematic review and meta-analysis. Resp Med 2011; 105: 1396-1403.

[4] Mondal A, Bhattacharya P, Saha G. Detection of lungs' status using morphological complexities of respiratory sounds. Sci World J 2014; Article ID 182938.

[5] Huq S, Moussavi Z. Acoustic breath-phase detection using tracheal breath sounds. Med Biol Eng Comput 2012; 50: 297-308.

[6] Tabata H, Hirayama M, Enseki M, Nukaga M, Hirai K, Furuya H, Mochizuki H. A novel method for detecting airway narrowing using breath sound spectrum analysis in children. Respir Investig 2016; 54: 20-28.

[7] Yahya O, Faezipour M. Automatic detection and classification of acoustic breathing cycles. In: IEEE 2014 Conference of the American Society for Engineering Education; 3–5 April 2014; Bridgeport, CT, USA. New York, NY, USA: IEEE. pp. 1-5.

[8] Dabiri S, Shirazi MAM. Estimation of respiratory rate from photoplethysmogram signal of sleep apnea patients: A comparative study of different methods. In: IEEE 2015 International Conference on Telecommunications and Signal Processing; 9–11 July 2015; Prague, Czech Republic. New York, NY, USA: IEEE. p. 440-443.

[9] Anusha AR, Soodi AL, Kumar SP. Design of low-cost hardware for lung sound acquisition and determination of inspiratory-expiratory phase using respiratory waveform. In: IEEE 2012 International Conference on Computing Communication and Networking Technologies; 26–28 July 2012; Coimbatore, India. New York, NY, USA: IEEE. p. 1-5.

[10] Moussavi ZK, Leopando MT, Pasterkamp H, Rempel G. Computerised acoustical respiratory phase detection without airflow measurement. Med Biol Eng Comput 2000; 38: 198-203.

[11] Nam Y, Reyes BA, Chon KH. Estimation of respiratory rates using the built-in microphone of a smartphone or headset. IEEE J Biomed Health 2015; 20: 1493-1501.

[12] Reyes BA, Reljin N, Kong Y, Nam Y, Ha S, Chon KH. Towards the development of a mobile phonopneumogram: automatic breath-phase classification using smartphones. Ann Biomed Eng 2016; 44: 2746-2759.

[13] Palaniappan R, Sundaraj K, Sundaraj S, Huliraj N, Revadi SS. A novel approach to detect respiratory phases from pulmonary acoustic signals using normalised power spectral density and fuzzy inference system. Clin Resp J 2016; 10: 486-494.

[14] Alsmadi S, Kahya YP. Design of a DSP-based instrument for real-time classification of pulmonary sounds. Comput Biol Med 2008; 38: 53-61.

[15] Lozano M, Fiz JA, Jané R. Performance evaluation of the Hilbert–Huang transform for respiratory sound analysis and its application to continuous adventitious sound characterization. Signal Proc 2016; 120: 99-116.

[16] Cam SL, Collet C, Salzenstein F. Acoustical respiratory signal analysis and phase detection. IEEE 2008 International Conference on Acoustics, Speech and Signal Processing; 31 March–4 April 2008; Las Vegas, NV, USA. New York, NY, USA: IEEE. pp. 3629-3632.

[17] Garcia D. Robust smoothing of gridded data in one and higher dimensions with missing values. Comput Stat Data An 2010; 54: 1167-1178.

[18] Rabiner L, Juang BH. Fundamentals of Speech Recognition. Upper Saddle River, NJ, USA: Prentice-Hall, 1993.

[19] Jin F, Sattar F, Goh D, Louis IM. A robust respiratory phase identification scheme based on a new mixing index. In: IEEE 2009 European Signal Processing Conference; 24–28 August 2009; Glasgow, UK. New York, NY, USA: IEEE, pp. 637-641.

[20] Yadollahi A, Moussavi ZM. A robust method for estimating respiratory flow using tracheal sounds entropy. IEEE T Biomed Eng 2006; 53: 662-668.